

RNA-Seq analysis of *Phanerochaete sordida*
YK-624 degrades neonicotinoid pesticide
acetamiprid

メタデータ	言語: eng 出版者: 公開日: 2022-02-04 キーワード (Ja): キーワード (En): 作成者: Wang, Jianqiao, Liu, Yilin, Yin, Ru, Wang, Nana, Xiao, Tangfu, Hirai, Hirofumi メールアドレス: 所属:
URL	http://hdl.handle.net/10297/00028578

**RNA-Seq analysis of *Phanerochaete sordida* YK-624 degrades neonicotinoid
pesticide acetamiprid**

Jianqiao Wang ^a, Yilin Liu ^a, Ru Yin ^a, Nana Wang ^a, Tangfu, Xiao ^a, Hirofumi Hirai ^b,
^{c*}

^a Key Laboratory for Water Quality and Conservation of the Pearl River Delta, Ministry of Education, School of Environmental Science and Engineering, Guangzhou University, Guangzhou 510006, China

^b Faculty of Agriculture, Shizuoka University, 836 Ohya, Suruga-ku, Shizuoka 422-8529, Japan

^c Research Institute of Green Science and Technology, Shizuoka University, 836 Ohya, Suruga-ku, Shizuoka 422-8529, Japan

* Corresponding author: Hirofumi Hirai

Mailing address: Faculty of Agriculture, Shizuoka University, 836 Ohya, Suruga-ku, Shizuoka 422-8529, Japan

Tel. & Fax: +81 54 238 4853

E-mail address: hirai.hirofumi@shizuoka.ac.jp

Abstract

1 Acetamiprid (ACE) belongs to the group of neonicotinoid pesticides, which have
2 become the most widely utilized pesticides around the world in the last two decades.
3 The ability of *Phanerochaete sordida* YK-624 to degrade ACE under ligninolytic
4 conditions has been demonstrated; however, the functional genes involved in ACE
5 degradation have not been fully elucidated. In the present study, the differentially
6 expressed genes of *P. sordida* YK-624 under ACE-degrading conditions and in the
7 absence of ACE were elucidated by RNA sequencing (RNA-Seq). Based on the gene
8 ontology enrichment results, the cell wall and cell membrane were significantly
9 affected under ACE-degrading conditions. This result suggested that intracellular
10 degradation of ACE might be mediated by this fungus. In addition, genes in metabolic
11 pathways were the most enriched upregulated differentially expressed genes
12 according to the KEGG pathway analysis. Eleven differentially expressed genes
13 characterized as cytochrome P450s were upregulated, and these genes were
14 determined to be particularly important for ACE degradation by *P. sordida* YK-624
15 under ligninolytic conditions.

Keywords: *Phanerochaete sordida* YK-624; acetamiprid; biodegradation; RNA-Seq;
cytochrome P450s

16

1. Introduction

17 Acetamiprid (ACE) is a neonicotinoid pesticide. Neonicotinoids are a relatively
18 new major group of pesticides that were developed in the 1990s. These pesticides are
19 selective agonists of nicotinic acetylcholine receptors (nAChRs), which bind more
20 strongly to nAChRs in insects than in vertebrates, causing receptor blockage, paralysis
21 and death at high concentrations [1-3]. Neonicotinoid pesticides have become the
22 most extensively utilized pesticides in the world with registration of over 140 crops in
23 more than 120 countries [4-5]. Although neonicotinoid pesticides are selective to pest
24 insects, recent studies suggest that they can also affect nontarget organisms, such as
25 pollinators and birds [6-7]. Neonicotinoids may affect the development of neurons
26 associated with such functions as learning and memory [8]. In recent years, some
27 studies have shown that neonicotinoid pesticides have similar excitatory effects on
28 mammalian developmental neurotoxicity [9]. Therefore, neonicotinoid pesticides
29 might be harmful to humans.

30 According to an analysis of 29 studies in 9 countries, neonicotinoids were
31 detected in 74% of surface waters [10]. Neonicotinoid pesticides have high water
32 solubility and can persist in soil for extended periods of time, leading to soil and water
33 contamination [11]. In recent years, a number of ACE degradation methods have been
34 reported. Heterogeneous photocatalysis and Fenton reaction degradation methods for
35 ACE have been reported [12-13]. Compared with chemical methods, microbial
36 degradation has the advantages of not producing secondary pollution and having low
37 cost. *Rhodotorula mucilaginosa* strain IM-2 selectively transformed ACE to
38 metabolite *N*-[(6-chloro-3-pyridyl)methyl]-*N*-methylacetamide (IM 1-3) through

39 hydrolysis [14]. The bacteria *Ensifer meliloti* CGMCC 7333, *Variovorax*
40 *boronicumulans* CGMCC 4969 and *Pseudaminobacter salicylatoxidans* CGMCC
41 1.17248 could degrade ACE, and the major metabolite was (*E*)-*N*²-carbamoyl-*N*¹-[(6-
42 chloro-3-pyridyl)methyl]-*N*¹-methylacetamide (IM 1-2) [15-17]. The bacteria
43 *Rhodococcus* sp. BCH2, *Pigmentiphaga* sp. AAP-1 and D-2 and *Stenotrophomonas*
44 sp. THZ-XP transformed ACE to *N*-methyl-(6-chloro-3-pyridyl)methylamine (IM 1-
45 4) [18-21]. The white-rot fungus *Phanerochaete sordida* YK-624 and the bacterium
46 *Stenotrophomonas maltophilia* CGMCC 1.1788 were able to demethylate ACE to
47 form (*E*)-*N*¹-[(6-chloro-3-pyridyl)-methyl]-*N*²-cyano-acetamide (IM 2-1) [22-23].
48 There are many studies describing ACE-degrading microorganisms and the
49 identification of ACE metabolites. However, the functional genes involved in the
50 degradation of ACE by *P. sordida* YK-624 have not been identified.

51 RNA sequencing (RNA-Seq) has gradually improved in the last ten years [24-
52 25]. The transcriptome is the link between genome and proteome information and
53 gene biological function. Therefore, the transcriptome has become an important tool
54 in molecular biology and plays an important role in understanding genomic function.
55 RNA-Seq is most commonly employed to analyse differentially expressed genes
56 (DEGs). In the present study, we utilized RNA-Seq to explore the DEGs of the white-
57 rot fungus *P. sordida* YK-624 under ACE-degrading conditions and in the absence of
58 ACE. The findings of this study may help to determine the functional genes involved
59 in the degradation of ACE by white-rot fungi.

2. Materials and methods

60 **2.1 Fungal culture conditions**

61 The strain *P. sordida* YK-624 (ATCC 90872) was preserved on potato dextrose
62 agar (PDA) at 4 °C. Next, the fungal disk was inoculated onto another PDA plate and
63 cultured at 30 °C for 3 d. Two fungal blocks with a diameter of 10 mm were drilled
64 out at the edge of the PDA plate and added to each 100-mL conical flask containing
65 10-mL Kirk medium, which was described by Kirk et al. [26]. The terminal
66 concentration of ACE was 10 µM, and the culture without ACE was used as a control.
67 Samples were harvested to perform RNA sequencing after 15 d of incubation (three
68 replicates). The ACE residue in the cultivation was quantified by high-performance
69 liquid chromatography (HPLC) using an InertSustain C18 column (4.6×150 mm; GL
70 Sciences, Japan). During the measurement, 30% methanol aq. was used as a mobile
71 phase and flowed in HPLC at a speed of 0.5 mL/min, and ACE was inspected at a
72 wavelength of 270 nm.

73 **2.2 Transcriptomic analysis and quantitative real-time PCR (qRT-PCR)**

74 The RNA isolation, cDNA library construction, and quantitative real-time PCR
75 methods are described in the Supplemental Materials. The library preparations were
76 sequenced on an Illumina Novaseq platform, and 150-bp paired-end reads were
77 generated. First, clean reads were obtained by removing low-quality reads, and the
78 reads containing adapter or ploy-*N* sequences from the raw data and Q20, Q30 and
79 GC content were calculated. No reference genome-based reads mapping was
80 performed in this study. After transcriptome assembly by Trinity, gene function was
81 annotated based on NCBI nonredundant protein sequences (Nr), NCBI nonredundant

82 nucleotide sequences (Nt), Swiss-Prot, Kyoto Encyclopedia of Genes and Genomes
83 (KEGG) and Gene Ontology (GO) databases. Differential expression analysis of the
84 **ACE_K** (Kirk medium with ACE) and **K_c** (control: Kirk medium without ACE)
85 samples was performed using the DESeq2 program [27]. The sample of mycelium
86 without ACE was regarded as the control. Genes with adjusted *P*-values < 0.05 and
87 log₂ fold changes > 1 were defined as differentially expressed. GO and KEGG
88 enrichment analyses of the DEGs were performed using the clusterProfiler R package
89 [28]. The read sequences were deposited in the NCBI Sequence Read Archive (SRA)
90 under accession number PRJNA690204.

91 RNA samples (1.5 µg) extracted as described in section 2.4 were used for the
92 reverse-transcriptase reaction, with the Hifair® II 1st strand cDNA synthesis kit
93 (Yeasen, Shanghai, China). qRT-PCR was performed using SYBR Green Master Mix
94 (Yeasen, China) on an ABI-Vii7 instrument (ABI, America). The amplification
95 reaction program was set as follows: predenaturation, 95 °C for 5 min; amplification,
96 40 cycles at 95 °C for 10 s and 60 °C for 30 s. After amplification, the temperature
97 was raised to 90 °C at a rate of 0.05 °C/s, and the melting curve was detected. *Actin*
98 was used as an internal reference to test the variations in the expression of upregulated
99 genes, and the primers used in this study are shown in [Table S1](#). Test results were
100 quantified by the 2^{-ΔΔCt} method [29].

101 **2.3 Evolutionary analysis of cytochrome P450**

102 The evolutionary history was determined by the neighbour-joining method
103 according to MEGA 7 [30-31]. Cluster-261.3684 was not used because its gene length

104 was short. The sum of branch length = 1049.39612815 is shown in the optimal tree.
105 The evolutionary distances were computed using the maximum composite likelihood
106 method and were presented in units of the number of base substitutions per site [32].
107 The codon positions included were 1st + 2nd + 3rd + noncoding. There were a total of
108 1250 positions in the final dataset.

3. Results and discussion

109 3.1 Overview of transcriptomic analysis

110 In our previous study, *P. sordida* YK-624 was able to degrade 45% ACE under
111 ligninolytic conditions after 15 d of incubation [22]. The degradation rate of ACE in
112 this study was similar to our previous result. To compare the results of this study with
113 the findings of previous research, samples cultured for 15 d were used in this study.
114 RNA-Seq was performed to study the transcriptome of *P. sordida* YK-624 under
115 ACE-degrading conditions and in the absence of ACE. The clean bases of **ACE_K**
116 (with ACE) were 11.4 Gb, 10.8 Gb, and 10.21 Gb, and those of **K_c** (without ACE)
117 were 9.93 Gb, 10.28 Gb, and 9.97 Gb, respectively (Table S2). The percentage of Q30
118 reached over 92.27% with a 0.02% error rate, and the GC contents were all
119 approximately 61% (Table S2). Based on adjusted *P*-values < 0.05 and log₂ fold
120 changes > 1, we identified 413 upregulated and 429 downregulated DEGs in ACE-
121 degrading conditions compared with the absence of ACE (Fig. 1). We used qRT-PCR
122 to test the biological reproducibility of the fold change obtained by RNA-Seq data.
123 Five upregulated genes in ACE-degrading conditions were selected to perform qRT-
124 PCR (Table S3). Similar trends regarding the expression levels of these genes were

125 obtained through qRT-PCR and RNA-Seq, thereby validating the reliability of the
126 RNA-Seq results (Fig. 2).

127 **3.2 GO and KEGG enrichment analysis of the DEGs of *P. sordida* YK-624**

128 DEGs were assigned to three categories in the GO enrichment analysis (correct
129 P -value < 1): 26 terms in biological process (BP), 9 terms in cellular component (CC),
130 and 5 terms in molecular function (MF), whereas no significantly enriched GO terms
131 were observed in upregulated DEGs. Among the BP categories, the top 5 enriched
132 terms were lipid biosynthetic, lipid metabolic, oxidation-reduction, cellular lipid
133 metabolic, and single-organism metabolic processes. Among the MF categories, the
134 most enriched terms were structural constituents of the cell wall, whereas the most
135 enriched terms were fungal-type cell walls in the CC category (Fig. 3). Lipids are
136 constituents of membranes in all organisms, and the fungal-type cell wall provides
137 protection from stresses and contributes to cell morphogenesis. Based on the GO
138 enrichment results, the cell wall and cell membrane of *P. sordida* YK-624 were
139 significantly affected under ACE-degrading conditions. This effect was probably
140 observed because injury to the cell wall and cell membrane of *P. sordida* YK-624
141 might be caused under ACE-degrading conditions. The cell membrane permeability of
142 *Stenotrophomonas maltophilia* was changed when benzo[α]pyrene was present, and
143 cell membrane ruptures were also observed [33]. White-rot fungi can secrete
144 ligninolytic extracellular peroxidases for lignin degradation and the three main types
145 of peroxidases, namely, lignin peroxidase, manganese peroxidases and versatile
146 peroxidases. Generally, only one upregulated DEG was characterized as lignin

147 peroxidase, and ligninolytic extracellular peroxidases played only minor roles in ACE
148 degradation by *P. sordida* YK-624. It has reported that ACE was *N*-demethylated to
149 (*E*)-*N*¹-[(6-chloro-3-pyridyl)-methyl]-*N*²-cyano-acetamidine (IM 2-1) by *P. sordida*
150 YK-624 [22]. This result suggested that the intracellular degradation of ACE might be
151 mediated by this fungus.

152 On the other hand, the KEGG enrichment analysis of the upregulated DEGs
153 showed that tryptophan metabolism, arginine and proline metabolism, inositol
154 phosphate metabolism, MAPK signalling pathway-yeast and thiamine metabolism
155 were the top 5 enriched genes. Relationships to metabolic pathways were the most
156 enriched in upregulated DEGs according to the KEGG pathway analysis (Fig. 4).

157 **3.3 ACE-degrading functional genes of *P. sordida* YK-624**

158 In our previous study, the degradation of ACE by *P. sordida* YK-624 was
159 observed to be affected by the addition of the cytochrome P450 inhibitor piperonyl
160 butoxide. Cytochrome P450 plays an important role in the degradation of ACE by *P.*
161 *sordida* YK-624 [22]. In the present study, 13 DEGs were characterized as
162 cytochrome P450 (Table S4). Cluster-261.1191, cluster-261.5282, cluster-261.6286,
163 cluster-261.3684, cluster-261.3747, cluster-261.2857, cluster-261.7977, cluster-
164 261.4980, cluster-261.5914, cluster-261.7094 and cluster-261.6823 were upregulated
165 2.02~3.14-fold in ACE-degrading conditions. Two genes (cluster-261.3761 and
166 cluster-261.1094) were downregulated. These results suggested that cytochrome
167 P450s played important roles in the degradation of ACE. The typical white-rot fungus
168 *P. chrysosporium*, which is the most extensively studied, has 156 cytochrome P450-

169 encoding genes in the genome [34]. Further evolutionary analysis of cytochrome
170 P450s in *P. chrysosporium* and 12 cytochrome P450-encoded genes in this study were
171 performed. Overall, cluster-261.2857, cluster-261.1191, and cluster-261.15914
172 exhibited a very close phylogenetic relationship, whereas cluster-261.6823, cluster-
173 261.4980, cluster-261.7977, cluster-261.7094 and cluster-261.1094 (downregulated)
174 were phylogenetically close. Cluster-261.3747, cluster-261.6286 and cluster-261.5282
175 were relatively close, while cluster-261.3761 (downregulated) was clearly separated
176 in the tree (Fig. 5). Recently, a cytochrome P450, CYP5147A3 (16 d) of *P.*
177 *chrysosporium*, was determined to be responsible for the degradation of ACE, and the
178 metabolites *N*'-cyano-*N*-methylacetamide and 6-chloro-3-pyridinemethanol were
179 identified [35]. CYP5147A3 (16 d) showed a distant phylogenetic relationship to the
180 cytochrome P450-encoding genes identified in this study (Fig. 5). This result may
181 explain why different metabolites were identified in *P. sordida* YK-624 and *P.*
182 *chrysosporium*.

183 According to the relevant literature, in the microbial degradation of ACE, only a
184 small number of ACE-degrading enzymes have been identified. Pure nitrile hydratase
185 (NHase) obtained from *E. meliloti* CGMCC 7333 could degrade 93.9% of ACE in the
186 reaction, and ACE was transformed to IM 1-2 [15]. In addition, a novel amidase,
187 AceAB, was purified from *Pigmentiphaga* sp. strain D-2; this enzyme played a major
188 role in the hydrolysis of ACE to IM 1-4 [36]. In this study, we did not detect NHase
189 and amidase among the upregulated DEGs. Some genes in the upregulated DEGs
190 were determined to encode oxidoreductases and dehydrogenases based on the Swiss-

191 Prot database. The genes that we obtained under ACE-degrading conditions should be
192 further heterologously expressed to confirm their functions.

Data Availability Statement

193 The datasets supporting the results of this article are deposited in the NCBI
194 database under accession number PRJNA690204.

Acknowledgement

195 The work was financially supported by the Research Project of Bureau of
196 Education of Guangzhou Municipality, China (no. 201831801).

References

- 197 1. Matsuda K, Buckingham SD, Kleier D, Rauh JJ, Grauso M, Sattelle DB.
198 Neonicotinoids: insecticides acting on insect nicotinic acetylcholine receptors.
199 Trends Pharmacol Sci. 2001; 22(11): 573-580.
- 200 2. Tomizawa M, Casida JE. Selective toxicity of neonicotinoids attributable to
201 specificity of insect and mammalian nicotinic receptors. Annu Rev Entomol.
202 2003; 48: 339-364.
- 203 3. Tomizawa M, Casida JE. Neonicotinoid insecticide toxicology: mechanisms of
204 selective action. Annu Rev Pharmacol Toxicol. 2005; 45: 247-268.
- 205 4. Bass C, Denholm I, Williamson MS, Nauen R. The global status of insect
206 resistance to neonicotinoid insecticides. Pestic Biochem Physiol. 2015; 121: 78-87.
- 207 5. Simon-Delso N, Amaral-Rogers V, Belzunces LP, Bonmatin JM, Chagnon M,
208 Downs C, Furlan L, Gibbons DW, Giorio C, Girolami V, Goulson D,
209 Kreutzweiser DP, Krupke CH, Liess M, Long E, McField M, Mineau P, Mitchell

- 210 EAD, Morrissey CA, Noome DA, Pisa L, Settele J, Stark JD, Tapparo A, Van
211 Dyck H, Van Praagh J, Van der Sluijs J, Whitehorn PR, Wiemers M. Systemic
212 insecticides (neonicotinoids and fipronil): trends, uses, mode of action and
213 metabolites. *Environ Sci Pollut Res Int.* 2015; 22: 5-34.
- 214 6. Basley K, Goulson D. Neonicotinoids thiamethoxam and clothianidin adversely
215 affect the colonisation of invertebrate populations in aquatic microcosms. *Environ.*
216 *Sci Pollut Res Int.* 2018; 25(10): 9593-9599.
- 217 7. Rundlöf M, Andersson GKS, Bommarco R, Fries I, Hederström V, Herbertsson L,
218 Jonsson O, Klatt BK, Pedersen TR, Yourstone J, Smith HG. Seed coating with a
219 neonicotinoid insecticide negatively affects wild bees. *Nature.* 2015; 521(7750):
220 77-80.
- 221 8. Kimura-Kuroda J, Komuta Y, Kuroda Y, Hayashi M, Kawano H. Nicotine-like
222 effects of the neonicotinoid insecticides acetamiprid and imidacloprid on
223 cerebellar neurons from neonatal rats. *PLoS One.* 2012; 7(2): e32432.
- 224 9. Christen V, Rusconi M, Crettaz P, Fent K. Developmental neurotoxicity of
225 different pesticides in PC-12 cells in vitro. *Toxicol Appl Pharmacol.* 2017; 325:
226 25-36.
- 227 10. Morrissey CA, Mineau P, Devries JH, Sanchez-Bayo F, Liess M, Cavallaro MC,
228 Liber K. Neonicotinoid contamination of global surface waters and associated risk
229 to aquatic invertebrates: A review. *Environ Int.* 2015; 74: 291-303.
- 230 11. Goulson D. An overview of the environmental risks posed by neonicotinoid
231 insecticides. *J Appl Ecol.* 2013; 50: 977-987.

- 232 12. Khan A, Haque MM, Mir NA, Muneer M, Boxall C. Heterogeneous
233 photocatalysed degradation of an insecticide derivative acetamiprid in aqueous
234 suspensions of semiconductor. *Desalination*. 2010; 261(1-2): 169-174.
- 235 13. Mitsika EE, Christophoridis C, Fytianos K. Fenton and Fenton-Like oxidation of
236 pesticide acetamiprid in water samples: kinetic study of the degradation and
237 optimization using response surface methodology. *Chemosphere*. 2013; 93: 1818-
238 1825.
- 239 14. Dai Y, Ji W, Chen T, Zhang W, Liu Z, Ge F, Yuan S. Metabolism of the
240 neonicotinoid insecticides acetamiprid and thiacloprid by the yeast *Rhodotorula*
241 *mucilaginosa* strain IM-2. *J Agric Food Chem*. 2010; 58(4): 2419-2425.
- 242 15. Zhou L, Zhang L, Sun S, Ge F, Mao S, Ma Y, Liu Z, Dai Y, Yuan S. Degradation
243 of the neonicotinoid insecticide acetamiprid via the N-carbamoylimine derivate
244 (IM-1-2) mediated by the nitrile hydratase of the nitrogen-fixing bacterium
245 *Ensifer meliloti* CGMCC 7333. *J Agric Food Chem*. 2014; 62(41): 9957-9964.
- 246 16. Sun S, Yang W, Guo J, Zhou Y, Rui X, Chen C, Ge F, Dai Y. Biodegradation of
247 the neonicotinoid insecticide acetamiprid in surface water by the bacterium
248 *Variovorax boronicumulans* CGMCC 4969 and its enzymatic mechanism. *RSC*
249 *Adv*. 2017; 7: 25387.
- 250 17. Guo L, Yang W, Cheng X, Fan Z, Chen X, Ge F, Dai Y. Degradation of
251 neonicotinoid insecticide acetamiprid by two different nitrile hydratases of
252 *Pseudaminobacter salicylatoxidans* CGMCC 1.17248. *Int Biodeter Biodegr*.
253 2021; 157: 105141.

- 254 18. Phugare SS, Jadhav JP. Biodegradation of acetamiprid by isolated bacterial strain
255 *Rhodococcus* sp. BCH2 and toxicological analysis of its metabolites in silkworm
256 (*Bombax mori*). Clean: Soil, Air, Water. 2015; 43(2): 296-304.
- 257 19. Tang H, Li J, Hu H, Xu P. A newly isolated strain of *Stenotrophomonas* sp.
258 hydrolyzes acetamiprid, a synthetic insecticide. Process Biochem. 2012; 47(12):
259 1820-1825.
- 260 20. Yang H, Wang X, Zheng J, Wang G, Hong Q, Li S, Li R, Jiang J. Biodegradation
261 of acetamiprid by *Pigmentiphaga* sp. D-2 and the degradation pathway. Int
262 Biodeter Biodegr. 2013; 85: 95-102.
- 263 21. Wang G, Yue W, Liu Y, Li F, Xiong M, Zhang H. Biodegradation of the
264 neonicotinoid insecticide acetamiprid by bacterium *Pigmentiphaga* sp. strain
265 AAP-1 isolated from soil. Bioresour Technol. 2013; 138: 359-368.
- 266 22. Wang J, Hirai H, Kawagishi H. Biotransformation of acetamiprid by the white-rot
267 fungus *Phanerochaete sordida* YK-624. Appl. Microbiol Biotechnol. 2012; 93:
268 831-835.
- 269 23. Chen T, Dai Y, Ding J, Yuan S, Ni J. N-demethylation of neonicotinoid
270 insecticide acetamiprid by bacterium *Stenotrophomonas maltophilia* CGMCC
271 1.1788. Biodegradation. 2008; 19(5): 651-658.
- 272 24. Emrich SJ, Barbazuk WB, Li L, Schnable PS. Gene discovery and annotation
273 using LCM-454 transcriptome sequencing. Genome Res. 2007; 17(1): 69-73.
- 274 25. Lister R, O'Malley RC, Tonti-Filippini J, Gregory BD, Berry CC, Millar AH,
275 Ecker JR. Highly integrated single-base resolution maps of the epigenome in

- 276 Arabidopsis. Cell. 2008; 133(3): 523-536.
- 277 26. Kirk TK, Schultz E, Connors WJ, Lorenz LF, Zeikus JG. Influence of culture
278 parameters on lignin metabolism by *Phanerochaete chrysosporium*. Arch
279 Microbiol. 1978; 117: 277-285.
- 280 27. Love MI, Huber W, Anders S. Moderated estimation of fold change and
281 dispersion for RNA-seq data with DESeq2. Genome Biol. 2014; 15(12): 550.
- 282 28. Yu G, Wang L, Han Y, He Q. clusterProfiler: an R package for comparing
283 biological themes among gene clusters. OMICS. 2012; 16(5): 284-287.
- 284 29. Livak K, Schmittgen T. Analysis of relative gene expression data using real-time
285 quantitative PCR and the 2⁻(-Delta Delta C(T)) Method. Methods. 2001; 25(4):
286 402-408.
- 287 30. Saitou N, Nei M. The neighbor-joining method: A new method for reconstructing
288 phylogenetic trees. Mol Biol Evol. 1987; 4: 406-425.
- 289 31. Kumar S, Stecher G, Tamura K. MEGA7: molecular evolutionary genetics
290 analysis version 7.0 for bigger datasets. Mol Biol Evo. 2016; 33(7): 1870-1874.
- 291 32. Tamura K, Nei M, Kumar S. Prospects for inferring very large phylogenies by
292 using the neighbor-joining method. PNAS. 2004; 101(30): 11030-11035.
- 293 33. Chen S, Yin H, Ye J, Peng H, Liu Z, Dang Z, Chang J. Influence of co-existed
294 benzo[a]pyrene and copper on the cellular characteristics of *Stenotrophomonas*
295 *maltophilia* during biodegradation and transformation. Bioresour Technol. 2014;
296 158: 181-187.
- 297 34. Hirosue S, Tazaki M, Hiratsuka N, Yanai S, Kabumoto H, Shinkyō R, Arisawa A,

- 298 Sakaki T, Tsunekawa H, Johdo O, Ichinose H, Wariishi H. Insight into functional
299 diversity of cytochrome P450 in the white-rot basidiomycete *Phanerochaete*
300 *chrysosporium*: Involvement of versatile monooxygenase. *Biochem Bioph Res*
301 *Co.* 2011; 407(1): 118-123.
- 302 35. Wang J, Ohno H, Ide Y, Ichinose H, Mori T, Kawagishi H, Hirai H. Identification
303 of the cytochrome P450 involved in the degradation of neonicotinoid insecticide
304 acetamiprid in *Phanerochaete chrysosporium*. *J Hazard Mater.* 2019; 371: 494-
305 498.
- 306 36. Yang H, Hu S, Wang X, Chuang S, Jia W, Jiang J. *Pigmentiphaga* sp. strain D-2
307 uses a novel amidase to initiate the catabolism of the neonicotinoid insecticide
308 acetamiprid. *Appl Environ Microbiol.* 2020; 86(6): e02425-19.

Figure Legends

Fig. 1 Volcano plot of DEGs in ACE_K (with ACE) versus K_c (without ACE) of *P. sordida* YK-624. Red plot: upregulated genes; green plot: downregulated genes; blue plot: nonsignificant genes.

Fig. 2 GO classification of DEGs of *P. sordida* YK-624. Blue: biological process (BP) categories; yellow: cellular component (CC); green: molecular function (MF) categories.

Fig. 3 KEGG pathway classification of upregulated genes involved in ACE degradation.

Fig. 4 Correlation analysis between qRT-PCR (histogram) and RNA-Seq (line) results for upregulated genes.

Fig. 5 Evolutionary relationships of cytochrome P450s. The analysis involved 168 nucleotide sequences. Codon positions included were 1st +2nd +3rd +Noncoding. All positions containing gaps and missing data were eliminated. Red: upregulated; blue: downregulated.

Supplementary material

Table S1 Primers used for qRT-PCR.

Table S2 Summary of transcripts information.

Table S3 Details of the five upregulated DEGs for qRT-PCR.

Table S4 Details of cytochrome P450 monooxygenase in the DEGs of *P. sordida* YK-624.

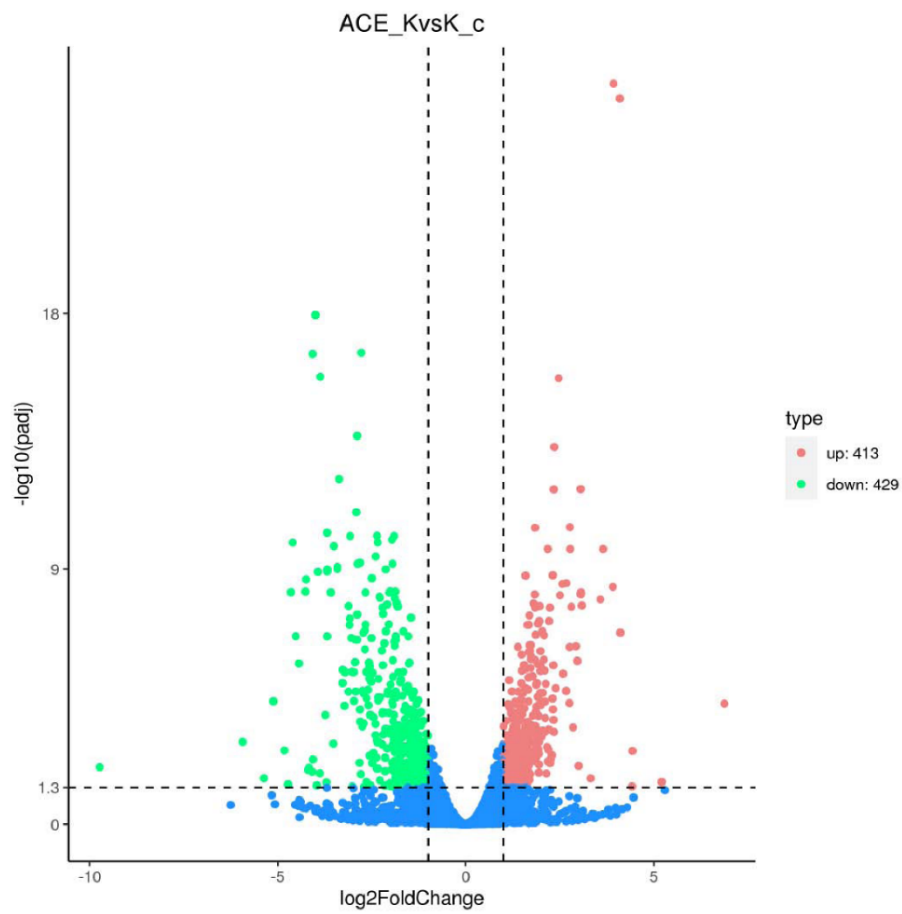


Fig. 1 Volcano plot of DEGs in ACE_K (with ACE) versus K_c (without ACE) of *P. sordida* YK-624. Red plot: upregulated genes; green plot: downregulated genes; blue plot: nonsignificant genes.

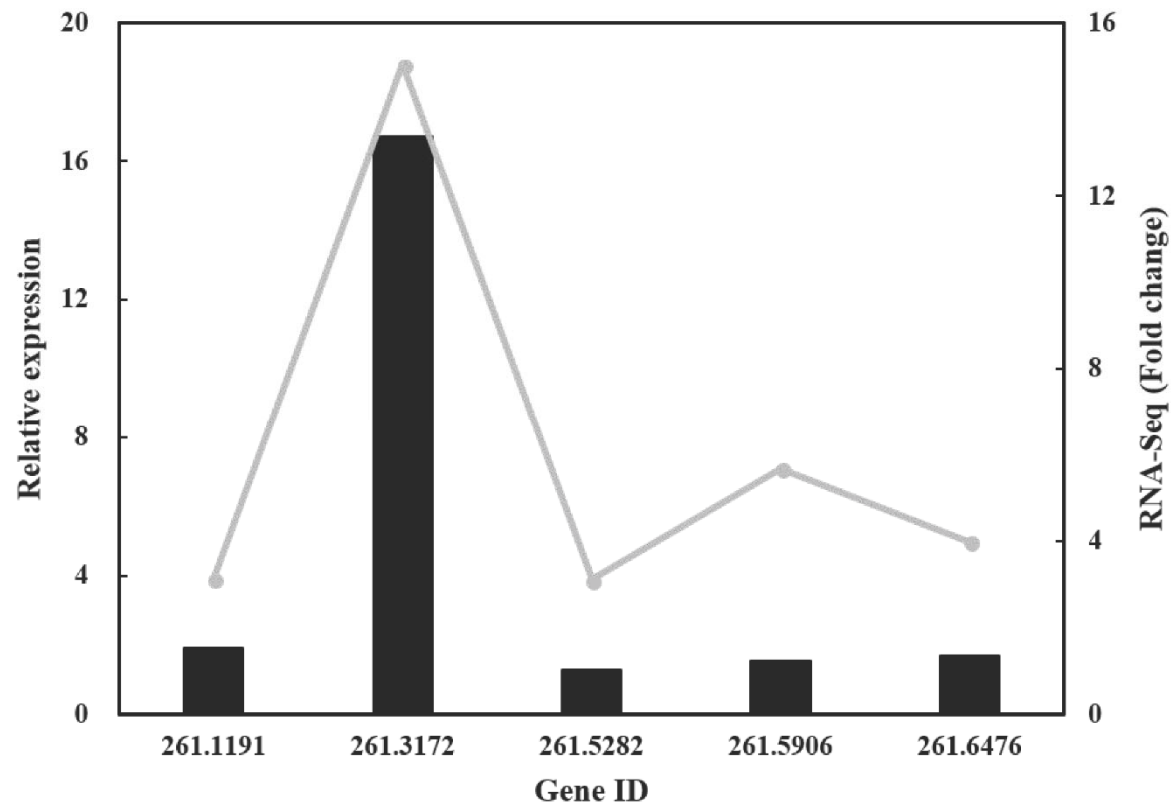


Fig. 2 Correlation analysis between qRT-PCR (histogram) and RNA-Seq (line) results for upregulated genes.

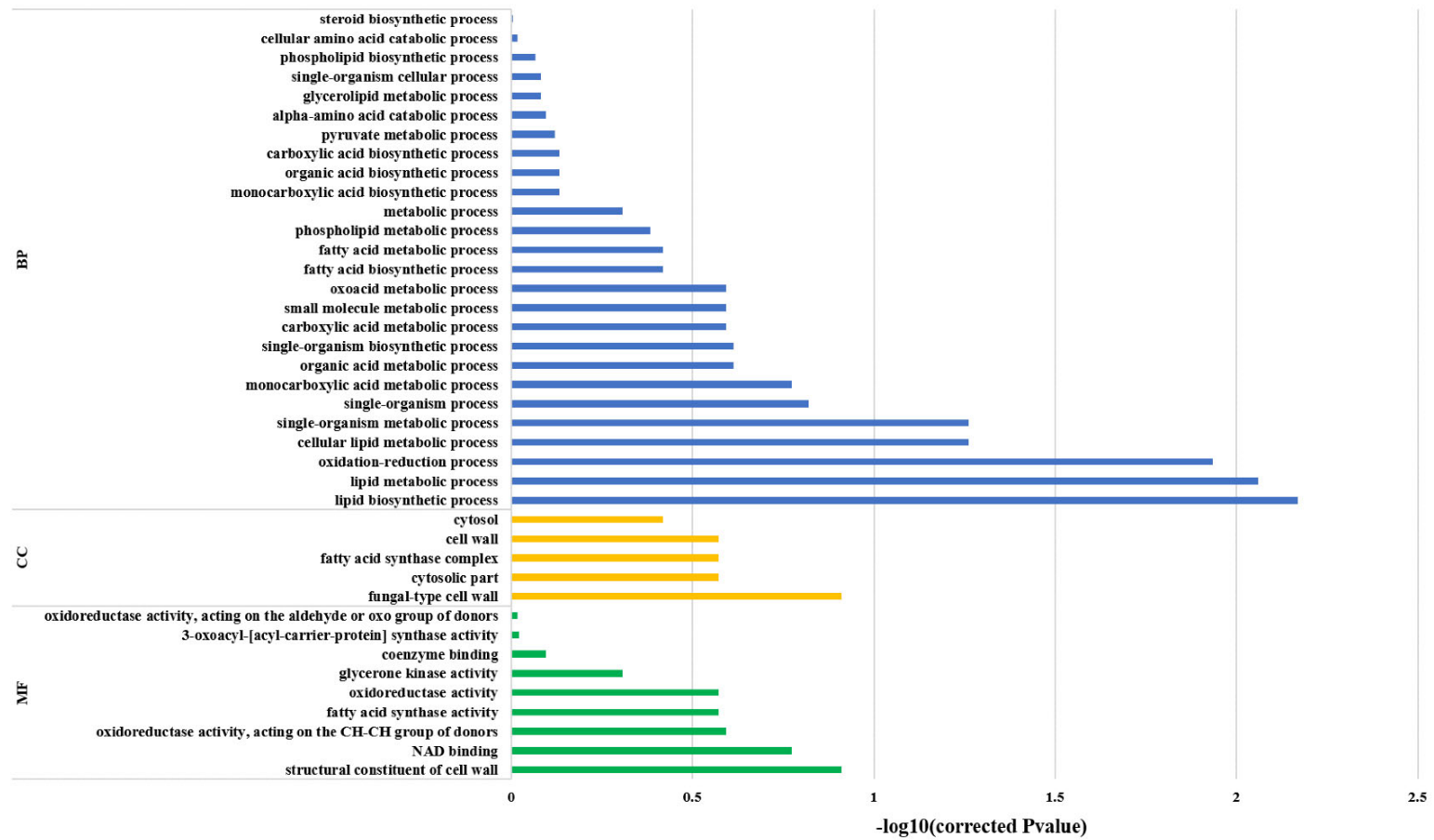


Fig. 3 GO classification of DEGs of *P. sordida* YK-624. Blue: biological process (BP) categories; yellow: cellular component (CC); green: molecular function (MF) categories.

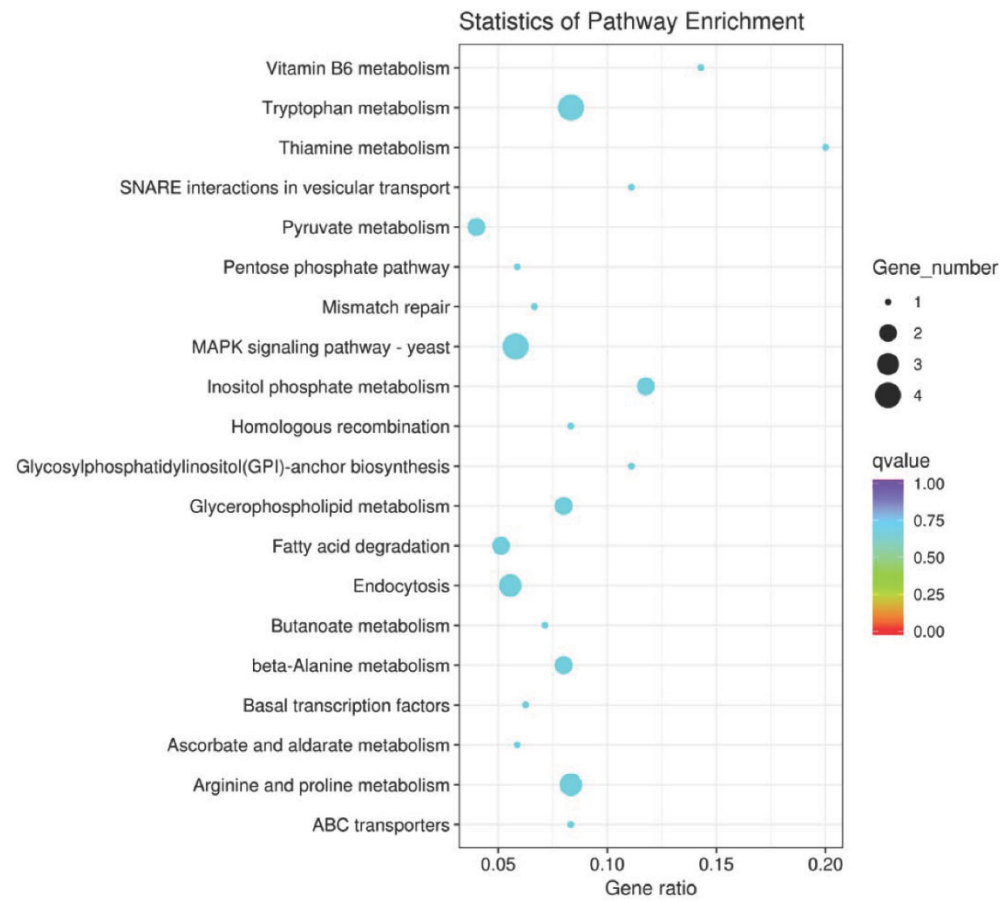


Fig. 4 KEGG pathway classification of upregulated genes involved in ACE degradation.

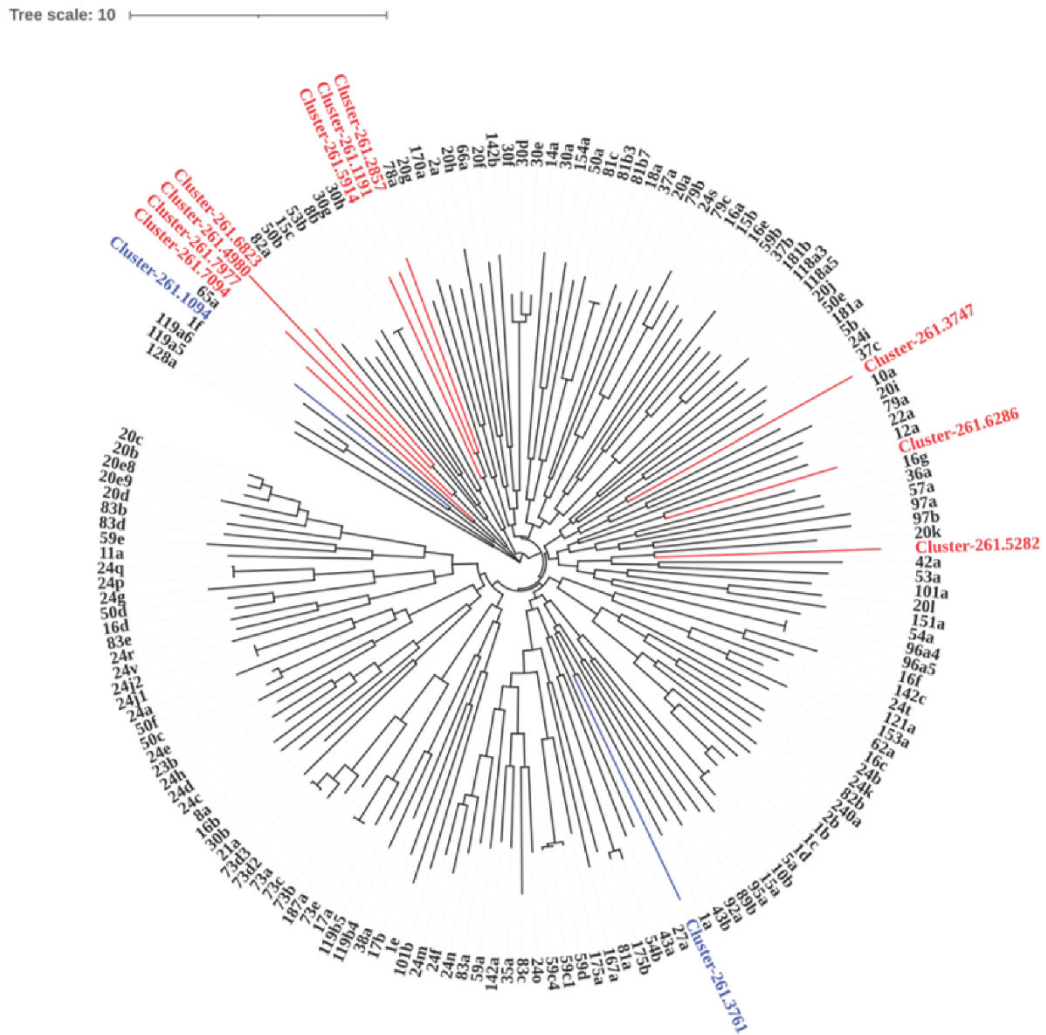


Fig. 5 Evolutionary relationships of cytochrome P450s. The analysis involved 168 nucleotide sequences. Codon positions included were 1st +2nd +3rd +Noncoding. All positions containing gaps and missing data were eliminated. Red: upregulated; blue: downregulated.

**RNA-Seq analysis of *Phanerochaete sordida* YK-624 degrades neonicotinoid
pesticide acetamiprid**

Jianqiao Wang ^a, Yilin Liu ^a, Ru Yin ^a, Nana Wang ^a, Tangfu, Xiao ^a, Hirofumi Hirai ^b,
^{c*}

^a Key Laboratory for Water Quality and Conservation of the Pearl River Delta, Ministry of Education, School of Environmental Science and Engineering, Guangzhou University, Guangzhou 510006, China

^b Faculty of Agriculture, Shizuoka University, 836 Ohya, Suruga-ku, Shizuoka 422-8529, Japan

^c Research Institute of Green Science and Technology, Shizuoka University, 836 Ohya, Suruga-ku, Shizuoka 422-8529, Japan

* Corresponding author: Hirofumi Hirai

Mailing address: Faculty of Agriculture, Shizuoka University, 836 Ohya, Suruga-ku, Shizuoka 422-8529, Japan

Tel. & Fax: +81 54 238 4853

E-mail address: hirai.hirofumi@shizuoka.ac.jp

Materials and methods

RNA isolation and cDNA library construction

Total RNA was extracted by RNAPrep Pure Plant Kit (DP441, TianGen, China) and the quality was assessed by the Bioanalyzer 2100 system (Agilent Technologies, CA, USA). For cDNA library construction, mRNA was purified from 1 µg total RNA and then fragmented using divalent cations. The first strand of cDNA was synthesized by M-MULV reverse transcriptase and random hexamer primer. The second strand of cDNA was synthesized from dNTPs by DNA Polymerase I system. The library fragments were filtered by AMPure XP system (Beckman Coulter, Beverly, USA) for cDNA fragments selection. The cDNA library was obtained after PCR amplification and then purified by AMPure XP system. Lastly, the quality of the cDNA library was Agilent 2100 Bioanalyzer and qRT-PCR used for assay.

Table S1 Primers used for qRT-PCR.

Primer	Sequence (5'-3')
261.1192-F	GGGTAGGCAGTCGAAGCAG
261.1192-R	TCGTCCCAACGATCCAAAGC
261.3172-F	AGCTTCCAGACTCGCCTCTA
261.3172-R	TTCACGCTGTTCTCGTTTGC
261.5282-F	GACGCGCATAGACGTACTIONA
261.5282-R	ACGTCCACACTTGCTCTCTG
261.5906-F	GTGCAGATAGGGGGAGGAGA
261.5906-R	ATCGAGGTTCCCTGGCTCAAC
261.6476-F	TGTGTCTTGTGCGCTGTAGT
261.6476-R	TCTCGTATGGGTCGGTCCTT
ActinF	AGCACGGTATCGTCACCAAC
ActinR	AGCGAAACCCTCGTAGATGG

Table S2 Summary of transcripts information.

Sample	Raw Reads	Clean Reads	Clean Bases	Error (%)	Q20 (%)	Q30 (%)	GC Content (%)
ACE_K_c1	34077422	33105452	9.93G	0.02	98.45	95.55	61.97
ACE_K_c2	36250896	34277777	10.28G	0.02	98.43	95.64	61.68
ACE_K_c3	35179092	33236392	9.97G	0.02	98.38	95.51	61.61
ACE_K1	38974305	37992959	11.4G	0.02	98.47	95.6	61.84
ACE_K2	37208058	36011948	10.8G	0.02	98.41	95.48	62.06
ACE_K3	35101066	34038581	10.21G	0.02	98.27	95.15	61.89

Table S3 Details of the five upregulated DEGs for qRT-PCR.

Gene_id	ACE_K readcount	ACE_K_c readcount	Log₂Fold Change	Pvalue	padj	Gene Length	Swiss-prot Description
Cluster- 261.3172	4213.2621 72	279.83648 85	3.9116	1.93E-11	4.25E-09	3327	Oxidoreductase ptaJ
Cluster- 261.5906	58258.055 95	10253.102 36	2.5064	4.77E-11	8.38E-09	5122	Dehydrogenase citC
Cluster- 261.6476	15179.940 34	3805.8387 79	1.9959	1.41E-06	6.25E-05	5870	Carboxylesterase B
Cluster- 261.1191	518.97072 74	164.95542 65	1.6528	2.26E-04	4.34E-03	2069	Cytochrome P450 monooxygenase FUM15
Cluster- 261.5282	815.75998 34	262.11546 7	1.638	8.07E-10	9.32E-08	3726	Cytochrome P450 monooxygenase FUM15

Log₂Fold change values of transcripts upregulated in ACE addition is represented by positive numbers and downregulated is represented by negative numbers.

Padj: adjust *P*-value

Table S4 Details of cytochrome P450 monooxygenase in the DEGs of *P. sordida* YK-624.

Gene_id	ACE_K readcount	ACE_K_c readcount	Log₂Fold Change	Pvalue	padj	Gene Length
Cluster- 261.1191	518.97072 74	164.95542 65	1.6528	0.00022579	0.0043409	2069
Cluster- 261.5282	815.75998 34	262.11546 7	1.638	8.07E-10	9.32E-08	3726
Cluster- 261.6286	1487.4563 22	498.17270 06	1.5783	2.73E-07	1.58E-05	2294
Cluster- 261.3684	63.816578 86	21.569511 35	1.5604	0.0022831	0.026072	430
Cluster- 261.3747	3479.5366 6	1194.0427 86	1.543	0.00040496	0.0068331	2560
Cluster- 261.2857	602.23945 42	226.80849 03	1.4075	3.88E-05	0.0010313	4057
Cluster- 261.7977	451.00553 59	176.05949 75	1.3557	0.00018763	0.0037126	1980
Cluster- 261.4980	6138.9863 43	2436.9011 9	1.3329	0.001496	0.018731	6664
Cluster- 261.5914	2210.3949 82	916.67368 79	1.2696	0.0022931	0.026123	4241
Cluster- 261.7094	2651.5234 59	1149.4526 61	1.2056	3.92E-05	0.0010376	9394
Cluster- 261.6823	308.57741 78	152.62394 3	1.0158	0.00084337	0.01213	2651
Cluster- 261.3761	482.64103 08	989.95265 78	-1.0361	0.0019228	0.022956	3780
Cluster- 261.1094	233.78145 96	518.58893 34	-1.1504	0.00032666	0.0058306	4566

Log₂Fold change values of transcripts upregulated in ACE addition is represented by positive numbers and downregulated is represented by negative numbers.

Padj: adjust *P*-value